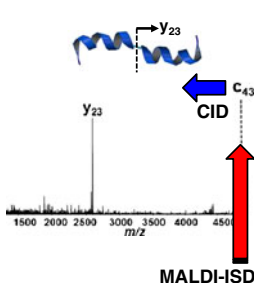**RESEARCH ARTICLE**

Selective and Nonselective Cleavages in Positive and Negative CID of the Fragments Generated from In-Source Decay of Intact Proteins in MALDI-MS

Mitsuo Takayama,[1] Sadanori Sekiya,[2] Ryunosuke Iimuro,[1] Shinichi Iwamoto,[2] Koichi Tanaka[2]

[1]Graduate School in Nanobioscience, Mass Spectrometry Laboratory, Yokohama City University, Kanazawa-ku, Yokohama, Japan
[2]Koichi Tanaka Laboratory of Advanced Science and Technology, Shimadzu Corporation, Nakagyo-ku, Kyoto, Japan

Abstract. Selective and nonselective cleavages in ion trap low-energy collision-induced dissociation (CID) experiments of the fragments generated from in-source decay (ISD) with matrix-assisted laser desorption/ionization mass spectrometry (MALDI MS) of intact proteins are described in both positive and negative ion modes. The MALDI-ISD spectra of the proteins demonstrate common, discontinuous, abundant c- and z'-ions originating from cleavage at the N–Cα bond of Xxx-Asp/Asn and Gly-Xxx residues in both positive- and negative-ion modes. The positive ion CID of the c- and z'-ions resulted in product ions originating from selective cleavage at Asp-Xxx, Glu-Xxx and Cys-Xxx residues. Nonselective cleavage product ions rationalized by the mechanism of a "mobile proton" are also observed in positive ion CID spectra. Negative ion CID of the ISD fragments results in complex product ions accompanied by the loss of neutrals from b-, c-, and y-ions. The most characteristic feature of negative ion CID is selective cleavage of the peptide bonds of acidic residues, Xxx-Asp/Glu/Cys. A definite influence of α-helix on the CID product ions was not obtained. However, the results from positive ion and negative ion CID of the MALDI-ISD fragments that may have long α-helical domains suggest that acidic residues in helix-free regions tend to degrade more than those in helical regions.

Key words: MALDI, In-source decay, Collision-induced dissociation, Protein

Introduction

Matrix-assisted laser desorption/ionization mass spectrometry (MALDI MS) [1, 2] is a powerful method for identifying proteins, while collision-induced dissociation (CID) coupled to electrospray ionization mass spectrometry (ESI MS) [3, 4] of enzymatic digestion products also presents a high-throughput tool for proteome analysis. Recent technologies such as MALDI MS combined with a tandem time-of-flight (TOF/TOF) [5, 6] and ion trap (IT) [7] have presented new perspectives in top-down proteomics by using low-energy CID coupled to a unique and specific cleavage method, namely "in-source decay (ISD)" [8, 9]. The MALDI-ISD/CID technique has been used to identify protein isoforms and disease biomarkers [10, 11], for imaging analysis [12], as well as to obtain sequence information from intact proteins without any digestion. It is expected that MALDI-ISD/CID of intact proteins may provide informative data reflecting their secondary structures (e.g., turn and helical regions). Here we report both positive and negative (pos/neg) ion CID of the ISD fragment c- and z'-ions (Schemes 1 and 2) generated from MALDI-ISD of intact proteins.

A recent interest of the MALDI-ISD concerns the study of backbone flexibility of proteins by means of hydrogen/deuterium exchange (HDX) with magnetic nuclear resonance (NMR) spectroscopy combined with MS [13]. In one research paper, the authors reported that amino acid residues susceptible to ISD in the protein equine cytochrome *c* were partly consistent with flexible amino acid residues as identified by HDX reaction with NMR [14], and that more preferential cleavage occurred at the N–Cα bond of Xxx-Asp/Asn and Gly-Xxx residues that are preferred in flexible

Correspondence to: Mitsuo Takayama; *e-mail:* takayama@yokohama-cu.ac.jp

secondary structures such as turns and bends than in other residues [15, 16]. Since the resulting ISD fragment c- and z′-ions originating from specific cleavage at Xxx-Asp/Asn and Gly-Xxx residues are abundant, it would seem to be advantageous to choose such intense peaks for performing CID experiments.

In contrast, there are a large number of research papers pertaining to the formation of b- and y-ions with low-energy CID of protonated peptides [17, 18]. The results obtained from a large amount of work performed by Wysocki and coworkers have resulted in general and principal rules for peptide fragmentation, i.e., a "mobile proton" [19] from protonated basic amino acid residues (Arg, Lys, and His) to amide nitrogen atoms on the backbone and a "charge remote" [20, 21] cleavage initiated with acidic hydrogen (or proton) of acidic amino acid residues (Asp, Glu, and Cys) [20–22]. Although the rules have been established for the CID of protonated peptides $[M + H]^+$, more work is needed to establish the CID behavior of deprotonated peptides $[M − H]^−$ and the influence of secondary structures on CID of peptide ions. There has been some effort to explain the generation of product ions from deprotonated peptides and comparison of pos/neg ion CID experiments [23–26]. With regard to the influence of secondary structures on CID, a study has been reported by Tsaprailis et al. in a paper describing positive ion CID characteristics in the presence of both acidic and basic amino acid residues in peptides [22], although it seems to be difficult to estimate the gas-phase secondary conformations such as α-helix and β-sheet of polypeptides.

In the present paper, low-energy ion trap CID experiments with c- and z′-ions generated from MALDI-ISD of intact proteins are described in order to compare the pos/neg ion CID characteristics. The proteins equine holo-cytochrome *c* and equine apo-myoglobin used contain 105 and 154 amino acids, respectively, and have primary, secondary, and tertiary structures as determined by X-ray crystallography and NMR spectroscopy and are recorded in the protein data bank (PDB). The CID experiments were performed for ISD fragment c- and z′-ions having definite secondary structures as judged by means of X-ray and NMR data. The resulting CID product ions are rationalized from the standpoint of the mechanisms of the "mobile proton" and the selective cleavages adjacent to acidic amino acid residues (Asp, Glu, and Cys) based on the "charge remote" mechanism. In particular, the negative ion CID products are explained by charge-mediated selective cleavage at Xxx-Asp/Glu/Cys residues, whereas positive ion products are explained by both mobile proton and charge remote mechanisms. It is suggested that there is a small influence of secondary structures such as an α-helix on the CID of the c- and z′-ions.

Experimental

Reagents

The MALDI matrix 5-amino-1-naphthol (5,1-ANL) was purchased from Tokyo Chemical Industry (Tokyo, Japan). Acetonitrile was purchased from Wako Pure Chemicals

(Osaka, Japan). Water used in all experiments was purified using a MilliQ water purification system from Millipore (Billerica, MA, USA). Equine holo-cytochrome *c* (Mr 12360.4) and equine apo-myoglobin (Mr 16951.4) were purchased from Sigma-Aldrich (Saint Louis, MO, USA). All reagents were used without further purification.

Protein and Matrix Preparations for MALDI-ISD Experiments

For the MALDI-ISD experiments, analyte protein was dissolved in water at a concentration of 20 pmol/μL. The matrix material was dissolved in water/acetonitrile (3:7, vol/vol) without any acid additives. A sample solution was prepared by mixing a volume of 10 μL of analyte solution with a volume of 10 μL of matrix solution. The molar ratio of analyte and matrix molecules was 1:1000. A volume of 0.5 μL of the sample solution was deposited onto a stainless-steel MALDI plate and the solvents were removed by allowing evaporation in air at room temperature.

MALDI Mass Spectrometry

MALDI-ISD spectrum was acquired on a time-of-flight mass spectrometer AXIMA-CFR (Shimadzu, Kyoto, Japan) equipped with a nitrogen laser (337 nm wavelength, 4 ns pulse width) operating at a pulse rate of 10 Hz. The laser spot size on the target substrate was ca. 100 μm in diameter. The ions generated by MALDI were accelerated using 20 kV with delayed extraction. The analyzer was operated in linear mode and the ions were detected using a microchannel plate detector. A total of 500 shots were accumulated for each mass spectrum acquisition. The reproducibility of each ISD spectrum was confirmed from the intensity patterns for several runs using the raster function installed on the AXIMA-CFR. MALDI-ISD/CID spectra were obtained with a quadrupole ion trap time-of-flight (QIT-TOF) mass spectrometer AXIMA Resonance (Shimadzu/Kratos, Manchester, UK) equipped with a nitrogen laser (337 nm wavelength, 3 ns pulse width) operating at a pulse rate of 10 Hz. The ISD fragment ions injected in the QIT were decelerated by a static electric field of 50 V applied to the far end-cap and collided with the pulsed argon gas for 30 ms. The product ions were extracted by applying a potential between the two end-caps and pulsed into the TOF system with an accelerating voltage of 10 kV.

Results and Discussion

Positive and Negative Ion MALDI-ISD Spectra of Intact Proteins

Here we use the notation for the ISD fragments as shown in Schemes 1 and 2. The notations c and z represent even electron neutral species, while c· and z· represent odd electron radical species (Scheme 1). With regard to the structure of even electron z′-ions we used here (Scheme 2), it
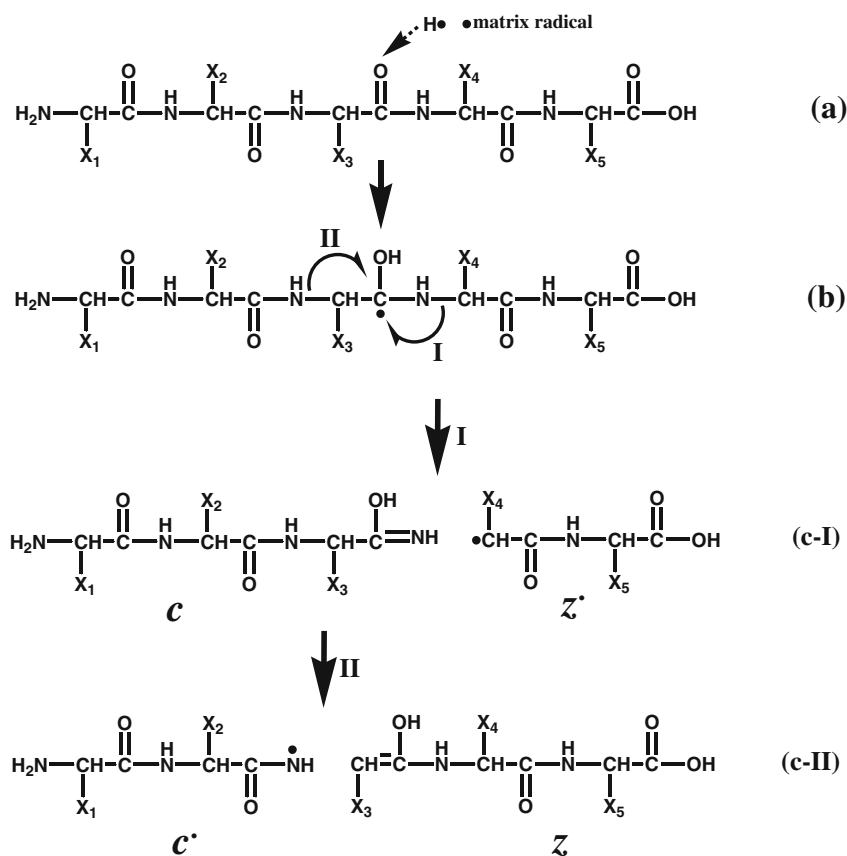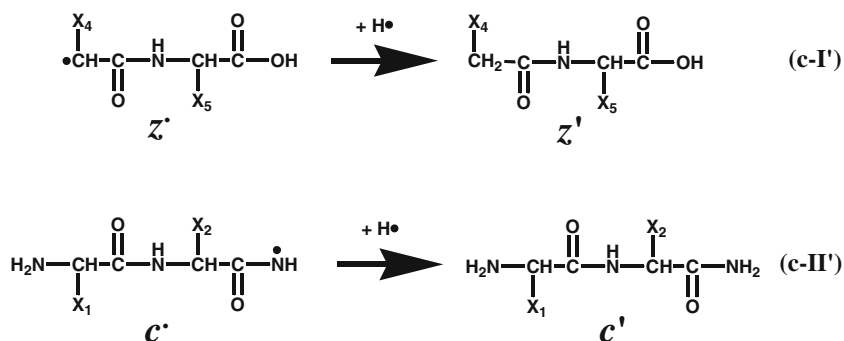
Scheme 1. Mechanism of the formation of c/z⁻ (dot) and c⁻(dot)/z pairs in MALDI-ISD

is likely that hydrogen radicals bind to the Cα position of odd electron radical species z⁻ as previously reported [27], because the radical z⁻-ion species were never observed here (data not shown). The preferential cleavage I, which gives z ′-ions, compared with II (Schemes 1 and 2) has been pointed out in a previous report [28]. Further, c-ion and z′-ion represent even electron protonated or deprotonated fragments (i.e., $[c + H]^+$, $[c – H]^-$, $[z′ + H]^+$, and $[z′ – H]^-$).

Both positive and negative (pos/neg) ion MALDI-ISD spectra of cytochrome c and myoglobin obtained with 5,1-ANL matrix [14, 29] are shown in Figures 1 and 2, respectively. In both Figures, the ISD spectra share something in common-discontinuous intense peaks of c- and z′-ions independent of

pos/neg ion modes. It should be noted that the peak abundance of the ISD fragment ions is governed by two factors: (1) the sites of charge, and (2) the susceptibility of amino acid residues to ISD. There is a general tendency that fragments including Arg or the amino (N)-terminus give abundant positive ion peaks, whereas those including carboxyl groups give relatively intense negative ion peaks [30]. In the MALDI-ISD spectra of cytochrome c (Figure 1), discontinuous intense fragment peaks and cleavage sites were c24 (Gly24-Xxx), c30 (Xxx-Asn31), c34 (Gly34-Xxx), c37 (Gly37-Xxx), c42 (Gln42-Xxx or Xxx-Ala43), c49 (Xxx-Asp50), c51 (Xxx-Asn52), c53 (Xxx-Asn54), c69 (Xxx-Asn70), z′14 (Glu90-Xxx or Xxx-Arg91), z′17 (Lys87-Xxx or Xxx-Lys88), and z′35 (Xxx-Asn70) in

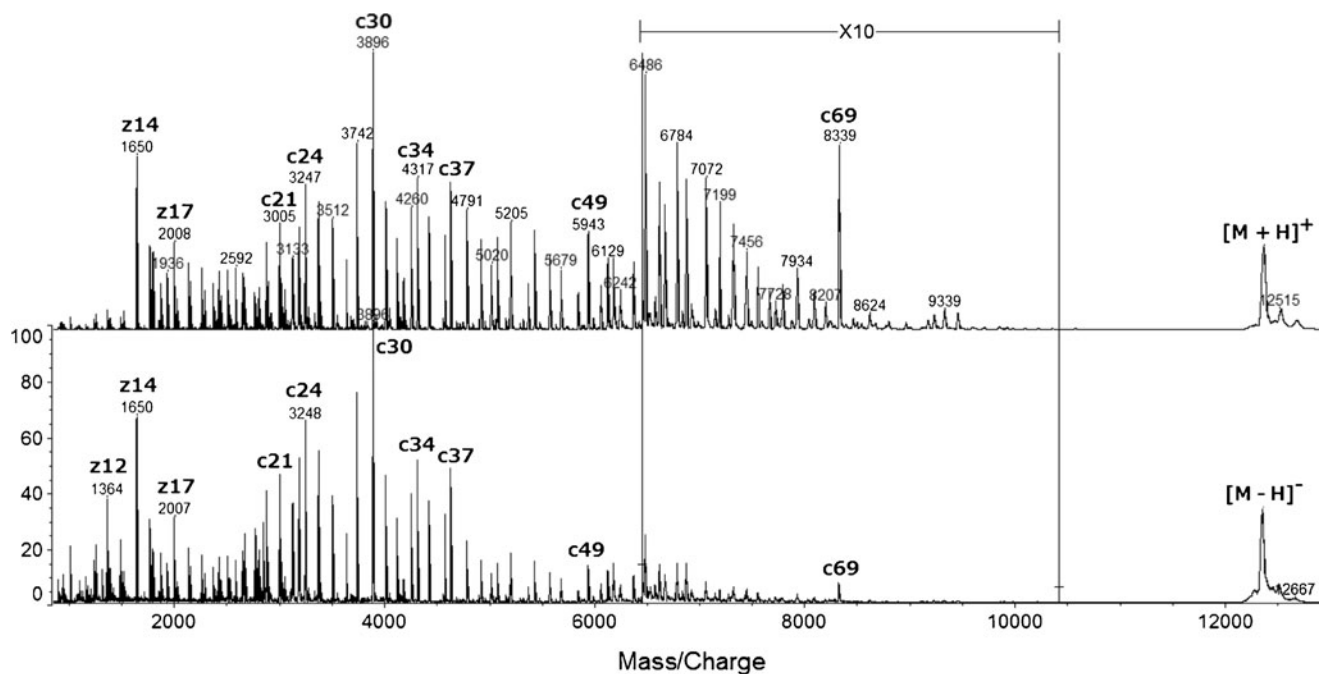**Scheme 2.** Mechanism of the formation of N-terminal side c′ and C-terminal side z′ fragments

Figure 1. Positive (upper) and negative (lower) ion MALDI-ISD spectra of equine holo-cytochrome c (Mr 12360.1) with 5-amino-1-naphtol (5,1-ANL) matrix

both pos/neg ions. In contrast, the intense fragments observed in the MALDI-ISD spectra of myoglobin were c19 (Xxx-Asp20), c23 (Gly23-Xxx), c25 (Gly25-Xxx), c35 (Gly35-Xxx), c43 (Xxx-Asp44), z′13 (Xxx-Asp141), z′15 (Phe138-Xxx or Xxx-Arg139), z′28 (Xxx-Asp126), and z′32 (Gly153-Xxx) in both pos/neg ions. From the ISD fragments obtained above, it was confirmed that the N–Cα bonds of Xxx-Asp/Asn

and Gly-Xxx residues are more susceptible than the other residues, with some exceptions such as z′14 and z′17 in cytochrome c and z′15 in myoglobin, independent of the pos/neg ions.

The susceptibility of the N-terminal side N–Cα bond of Asp and Asn residues, Xxx-Asp/Asn, and the C-terminal side of the Gly residue, Gly-Xxx, may be related to the secondary structures
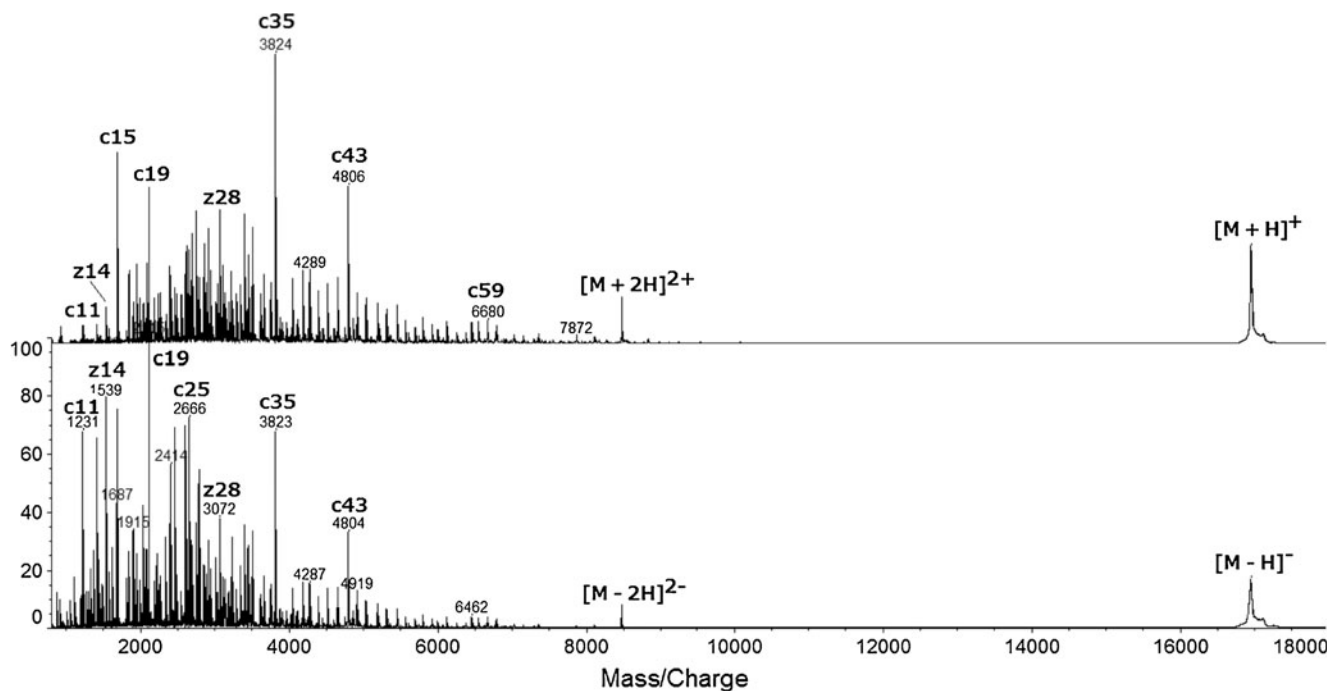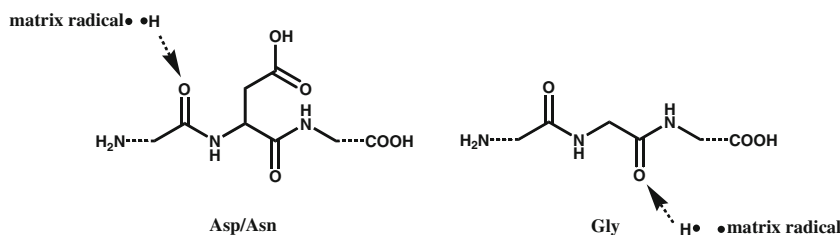

Figure 2. Positive (upper) and negative (lower) ion MALDI-ISD spectra of equine apo-myoglobin (Mr 16951.4) with 5-amino-1-naphtol (5,1-ANL) matrix

Scheme 3. Carbonyl oxygens preferred for binding hydrogen radicals

of the proteins. It has been reported that Asp, Asn, Gly, Pro, and Ser residues are preferred in flexible secondary structure (turn) rather than in intramolecular hydrogen-bonded structures such as helix and sheet, and Pro, Gly, Ser, Cys, and Tyr residues tend to destroy the formation of a helix [31, 32]. The helix structure may protect backbone carbonyl oxygens from attachment of hydrogen radicals and the formation of hypervalent radical species (Scheme 1), so that the carbonyl oxygens at the N-terminal side of Asp and Asn residues and those at the C-terminal side of Gly residues are expected to be more exposed to hydrogen radicals or matrix molecules than the other residues (Scheme 3). The discontinuous intense peaks of $c24$, $c30$, $c34$, $c37$, $c42$, $c49$, $c69$, $z'17$, and $z'35$ ions for cytochrome c (Figure 1) originate from the amino acid residues lying in helix free regions as judged from study of X-ray crystallography [PDB: 1CRC] and NMR spectroscopy [PDB: 1AKK] derived structures, although $z'14$, $c51$ and $c53$ ions are in helical domains. The complementary $c69/z'35$ pair ions originate from the N–Cα bond cleavage at the Xxx-Asn70 residue. For myoglobin (Figure 2), the intense peaks of $c19$, $c35$, $c43$, and $z'28$ ions originate from N–Cα bond cleavage at Xxx-Asp and Gly-Xxx residues in helix free regions as judged by study of the X-ray crystallography derived structure [PDB: 2FRF], whereas $c23$ and $c25$ ions come from helical domains. The results obtained above imply that Xxx-Asp/Asn and Gly-Xxx residues, which are preferentially found in flexible secondary structures, such as turn and bend, are susceptible to MALDI-ISD independent of both pos/neg ions. The appearance of discontinuous intense peaks of c- and z'-ions is useful for rapidly identifying the sites of Asp/Asn and Gly residues on the backbone, and for choosing the precursor ions for subsequent CID experiments.

Pos/Neg Ion CID Characteristics of c'- and z'-Ions from MALDI-ISD of Cytochrome c

Positive and negative (pos/neg) ion CID spectra of discontinuous intense fragments c- and z'-ions observed in the MALDI-ISD spectra of intact holo-cytochrome c were obtained for $c30$, $z'14$, and $z'35$ ions, and the resulting relatively abundant product b- and y-ions (b-/y-ions) are summarized in Table 1, together with cleavage sites and relative intensity. Figure 3 shows the pos/neg ion CID spectra of the C-terminal side $z'35$ ion originating from cleavage at the N–Cα bond of the

Xxx-Asn70 residue. The positive ion CID spectrum showed b-/y-ions originating from cleavage at the peptide bond of Asp/Glu-Xxx and/or Xxx-Glu residues. The $b21$/$y14$ ions are a complementary pair originating from cleavage at Glu21-Arg22. The negative ion CID spectrum showed the peaks corresponding to the loss of neutrals NH_3 and/or H_2O from the b-/y-ions originating from cleavages adjacent to acidic amino acid residues. The neutral loss from the b-/y-ions in negative ion CID has been described by Pu et al. [25]. The positive ion CID spectrum of the $c30$ ion with heme between Cys14 and Cys17 showed b-/y-ions originating from the loss of heme and peptide bond cleavage at Xxx-Cys and Asp/Glu-Xxx residues accompanied by the loss of H_2S (from cysteine) and H_2O (Supplemental Figure S1). The product ion at m/z 1819 originated from cleavage at Xxx-Cys17 and can be assigned as the $c16$ ion (Supplemental Figure S1). Although the negative ion CID of the $c30$ ion made it difficult to assign the product ions, the successive losses of neutrals such as H_2O, NH_3, H_2S, and/or CH_3COH (from threonine) from b-, y-, and c-ions would lead to the possible product ions. The formation of c-ions in low energy CID of peptides has been proposed by Harrison and Young [33]. It is likely that in the negative ion CID, the

Table 1. Product Ions, Cleavage Sites, and Relative Intensity (%) Observed in Positive and Negative Ion CID Spectra of the Discontinuous Intense Fragment Ions c- and z'-Ions Generated in the MALDI-ISD of Intact Holo-Cytochrome c

Precursor	Product ions (cleavage residues, relative intensity %)
c30: GDVEKGKKIFVQKCAQCHTVEKGGKHKTGP with heme in Cys14 and Cys17	
Pos: y14 (Q-C, 100)*, c16 (Q-C, 80), y28 (D-V, 60), b21 (E-K, 50), b13 (K-C, 50)	
Neg: c13 (K-C, 100)*, y29/y14 (G-D/K-C, 100)*, c16/y29 (Q-C/G-D, 36)*, c16 (Q-C, 34)*	
z14: EREDLIAYLKKATNE	
Pos: b3 (D-L, 100), b13 (N-E, 65), b6 (A-Y, 43), b9 (K-K, 38), b5 (I-A, 38), b4 (L-I, 34), b10 (K-A, 32)	
Neg: y12 (E-D, 100)*, y12/b13 (E-D/N-E, 30), b13 (N-E, 20)*	
z35: NPKKYIPGTKMIFAGIKKKTEREDLIAYLKKATNE	
Pos: b24 (D-L, 100), y14 (E-R, 38), b23 (E-D, 35), b21 (E-R, 35), b34 (N-E, 24), b22(R-E, 20)	
Neg: y12 (E-D, 100)*, y13 (R-E, 70)*, b34/y12 (N-E/E-D, 36)*	

* Accompanied with the loss of neutrals such as NH_3, H_2O, H_2S (from Cys), and/or CH_3COH (from Thr)

Figure 3. Positive (upper) and negative (lower) ion CID spectra of the fragment z′35 ion generated from MALDI-ISD of equine holo-cytochrome c

product ions observed are originated from the cleavage at Xxx-Cys14 and Xxx-Cys17 with neutral losses. The product ions observed in the pos/neg ion CID spectra of the c30 and z′35 ions generated from the ISD of cytochrome c could be explained by the charge remote mechanism on the basis of selective cleavages adjacent to acidic residues Asp, Glu, and Cys, as was previously reported [17, 22].

In contrast, the positive ion CID spectrum of the z′14 ion showed a series of b-ions originating from nonselective cleavages suggesting the mobile proton mechanism originating from the protonated N-terminus or Arg2 residue, as well as the mechanism of preferential cleavage adjacent to acidic residues (Figure 4) play a role. In the case of negative ion CID of the z′14 ion, however, the product ions observed were almost limited to cleavages adjacent to acidic Asp/Glu residues. The results described above suggest that negative ion CID of the MALDI-ISD fragments of protein results in product ions originating from cleavage adjacent to acidic residues.
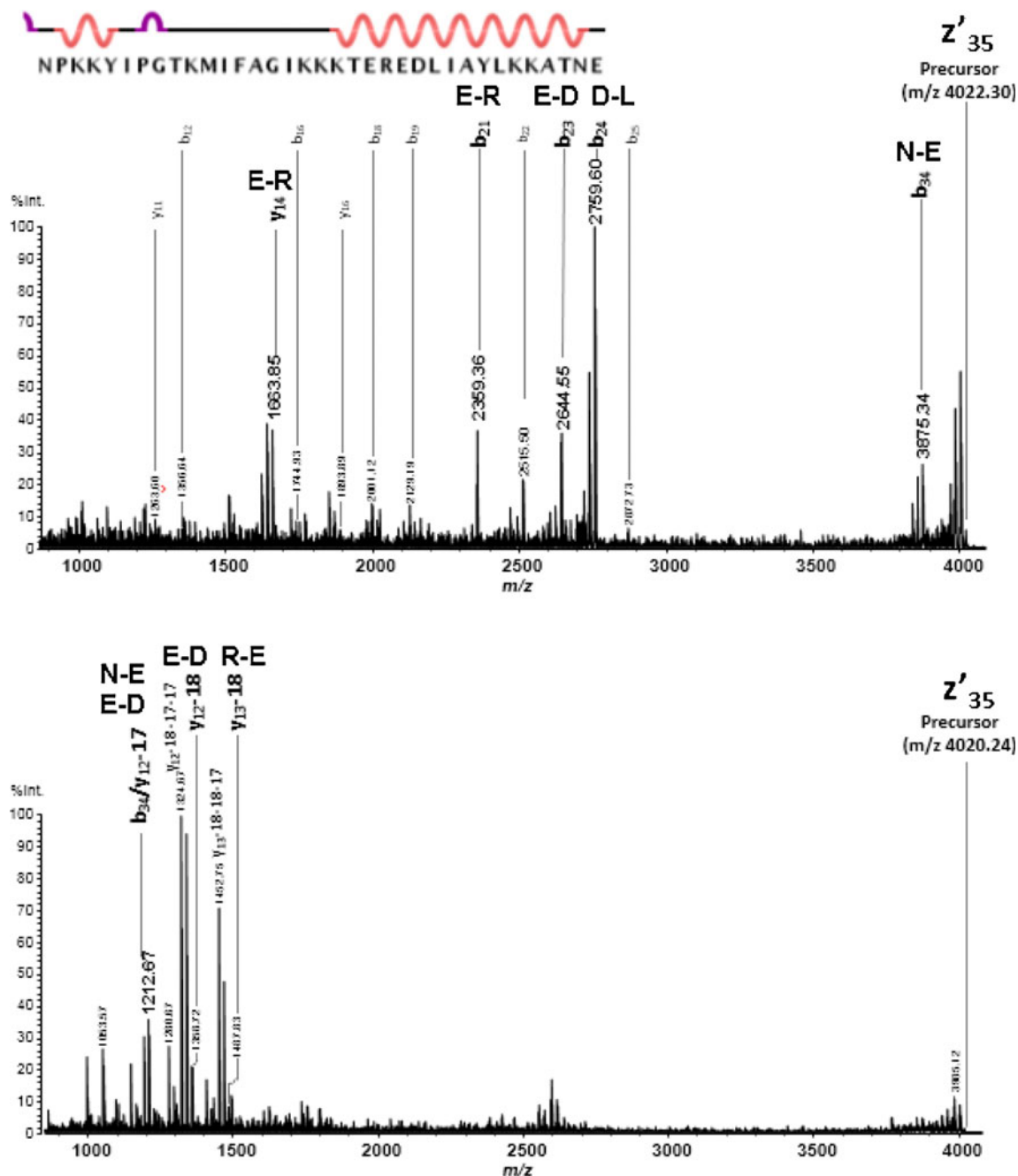
Figure 4. Positive (upper) and negative (lower) ion CID spectra of the fragment z′14 ion generated from MALDI-ISD of equine holo-cytochrome *c*

Pos/Neg Ion CID Characteristics of c- and z'-Ions from MALDI-ISD of Myoglobin

Pos/neg ion CID spectra of the discontinuous abundant c- and z′-ions observed in the MALDI-ISD spectra of intact apo-myoglobin were obtained for c35, c43, z′15, and z′28 ions. The resulting b-/y-ions, cleavage sites and relative intensity are summarized in Table 2. Figure 5 shows a positive ion CID spectrum of the C-terminal side c43 ion originating from

cleavage at the N–Cα bond between Phe43 and Asp44. The CID spectrum shows a strikingly abundant product ion y23 originating from cleavage of the peptide bond between residues Asp20 and Ile21. The positive ion CID of c35 also showed an abundant product ion y15 originating from the same Asp20 and Ile21 residues (data not shown). However, negative ion CID spectra of the ISD ions of c43 and c35 did not show any readable product ions (Supplemental Figure S2), whereas the negative ion CID spectra of other ISD fragment ions of

Table 2. Product Ions, Cleavage Sites, and Relative Intensity (%) Observed in Positive and Negative Ion CID Spectra of the Discontinuous Intense Fragment Ions c- and z′-Ions Generated in the MALDI-ISD of Intact apo-Myoglobin

Precursor	Product Ions (cleavage residues, relative intensity %)
c35: GLSDEGWQQVLNVWGKVEADIAGHGQEVLIRLFTG	
	Pos: y15 (D-I, 100), y8 (E-V, 15), y17 (E-A, 12), y31 (D-G, 10)
	Neg: No readable product ions.
c43: GLSDEGWQQVLNVWGKVEADIAGHGQEVLIRLFTGHPETLEKF	
	Pos: y23 (D-I, 100), y16 (E-V, 20), y39 (D-G, 10), y25 (E-A, 8)
	Neg: No readable product ions.
z15: RNDIAAKYKELGFQG	
	Pos: b10 (E-L, 74), b9 (K-E, 72), y12 (D-I, 72), b6 (A-K, 64), b7 (K-Y, 58), b4 (I-A, 56), y13 (N-D, 44)
	Neg: y13 (N-D, 100)*, y6 (K-E, 46)*
z28: DAQGAMTKALELFRNDIAAKYKELGFQG	
	Pos: b16 (D-I, 100), b16/y27 (D-I/D-A, 58), b15 (N-D, 48), y27 (D-A, 36), b14 (R-N, 34), y17 (E-L, 30)
	Neg: y13 (N-D, 100)*, b15 (N-D, 20)*

* Accompanied with the loss of neutrals such as NH_3, H_2O, and/or CH_3COH (from Thr)

myoglobin (Table 2 and Figure 6) and cytochrome c showed product ions corresponding to the loss of neutrals from b-/y-ions originating from cleavage adjacent to acidic residues. The relationship between the ISD fragment ions c35 and c43 and the structural characteristics of the peptides is that the Asp20 residue exists in a helix-free region between two helical domains Asp4-Ala19 and Ile21-Gly35. The resulting positive CID product y-ions from the ISD fragment ions c35 and c43 can be understood by means of selective cleavage at Asp/Glu-Xxx residues and protonated Arg31, although the products y16, y39, and y25 for

c43 in Table 2 were considerably lower in abundance than the product ion y23. Furthermore, the positive ion CID of the z′15 ion showed b4, b6, and b7 product ions originate from nonselective cleavage by means of the mobile proton mechanism from the protonated N-terminus or Arg residue, while negative ion CID showed that the products were due to selective cleavage at Xxx-Asp/Glu residues (data not shown). Figure 6 shows pos/neg ion CID spectra of the ISD fragment z′28 ion. The negative product ions observed can be explained by selective cleavage adjacent to acidic Asp/Glu residues and the loss of neutrals from b-/y-ions, although the positive ion product b14 ion can be explained by the mobile proton mechanism. The negative product b15 and y13 ions are a complementary pair originating from cleavage at Asn-Asp residues.

Selective Cleavage at Xxx-Asp/Glu/Cys Residues

Positive ion low-energy CID spectra of the fragment c- and z′-ions generated from the MALDI-ISD of intact proteins demonstrated the presence of product b-/y-ions which could be rationalized by the mobile proton mechanism or selective cleavage at Asp/Glu-Xxx with other cleavage sites such as at Xxx-Cys and Xxx-Asp/Glu residues. The selective cleavages adjacent to acidic residues are caused by an interaction or attack of acidic hydrogen (or proton) on the amide backbone (Scheme 4) [16, 21]. In contrast, the negative ion CID results in product ions originating from cleavage at the N-terminal side of peptide bonds of Asp/Asn/Cys residues (i.e., Xxx-Asp/Glu/Cys) with the loss of neutrals. It is noteworthy that the negative ion cleavages adjacent to the acidic residues are almost always
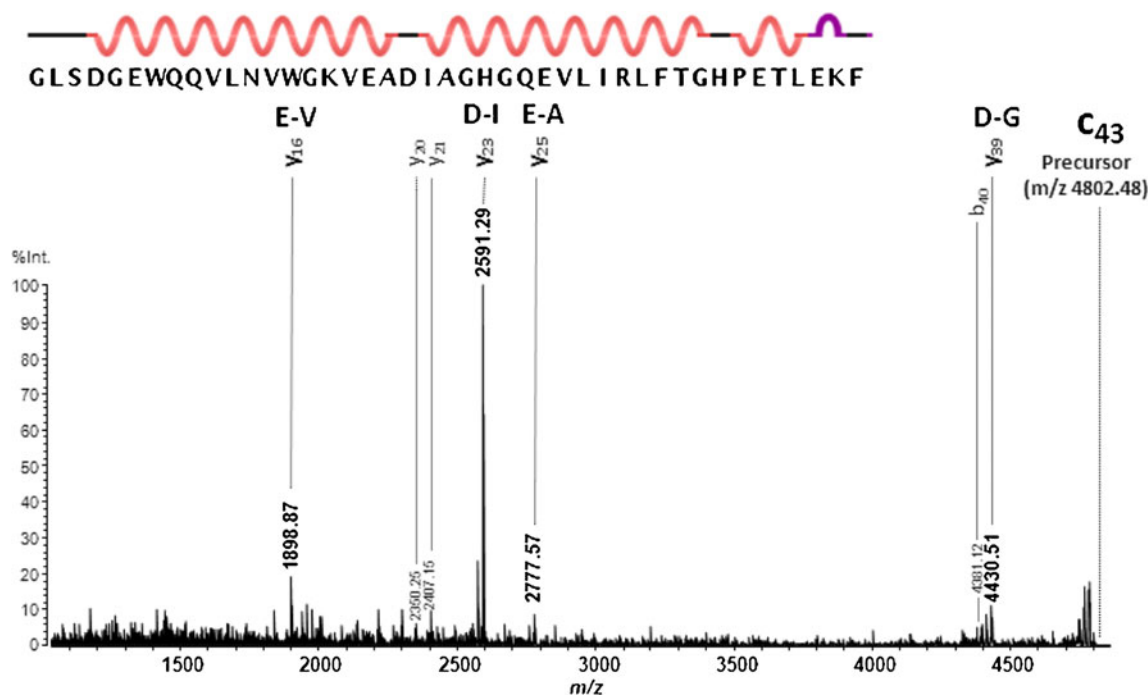

Figure 5. Positive ion CID spectrum of the fragment c43 ion generated from MALDI-ISD of equine apo-myoglobin
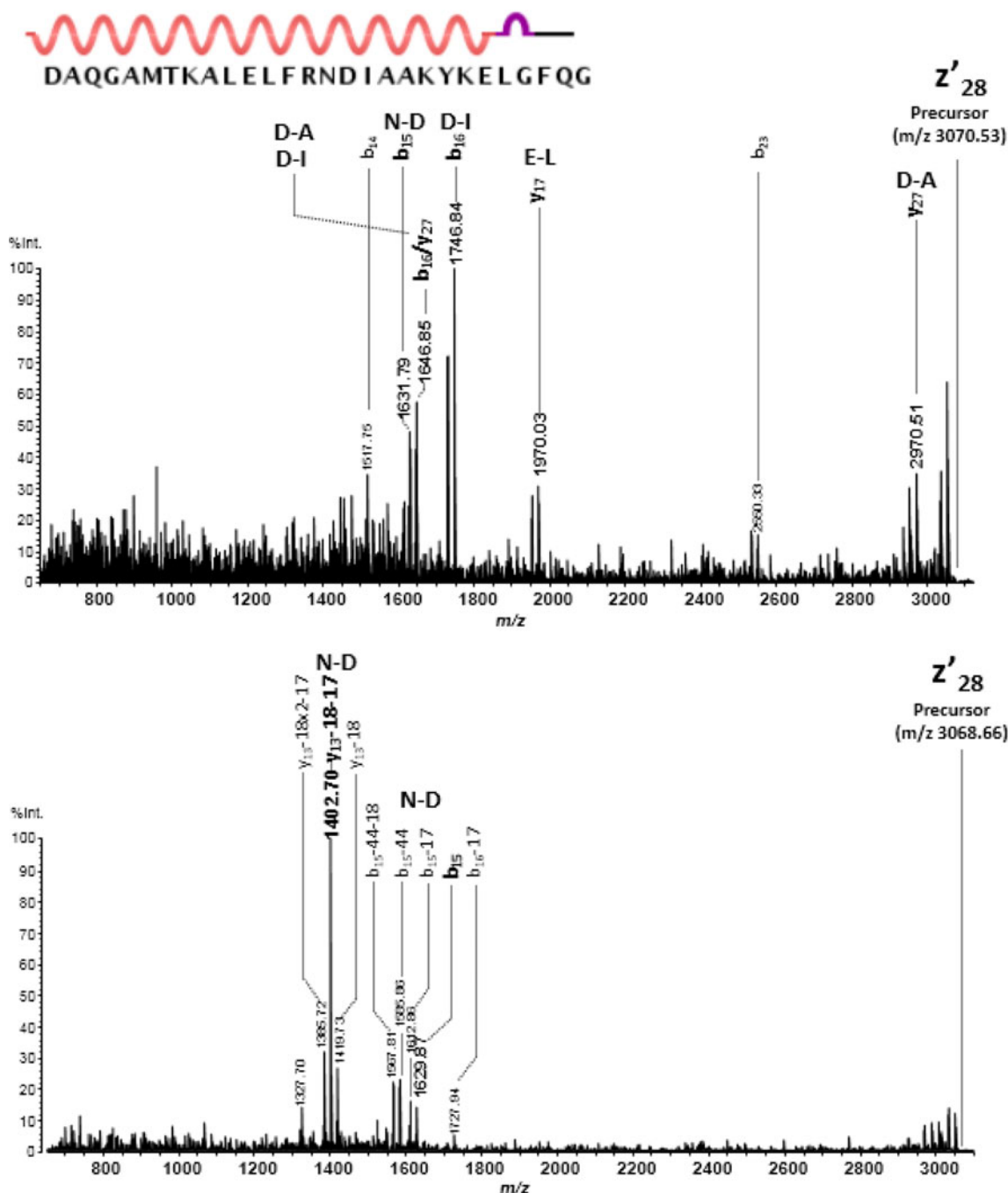
Figure 6. Positive (upper) and negative (lower) ion CID spectra of the fragment z′28 ion generated from MALDI-ISD of equine apo-myoglobin

limited to the N-terminal side of those residues, which in positive ion CID produce cleavages at both N- and C-terminal sides. Bowie et al. [23] and Harrison [24] have proposed that charge-mediated cleavage of the backbone take place, followed by the transfer of negative charge from C-terminal carboxyl oxygen to the internal backbone regions. When the negative charge transfer from the C-terminus to the backbone occurs, it is likely that the negative charge is preferentially located on the acidic Asp/Glu/Cys residues, and that a charge-mediated

cleavage of the backbone may occur to generate the product b-/y-ions (Scheme 5), accompanied by the loss of neutrals. The hydrogen rearrangements from the α-carbon on the backbone have been proposed by Bowie et al. [23] and Harrison et al. [34]. O'Connor et al. have reported that in an electron capture dissociation (ECD) experiment of peptides, radical-mediated scrambling of the deuterium atoms of the α-carbon takes place before the final cleavage and generation of the detected fragment ions [35].
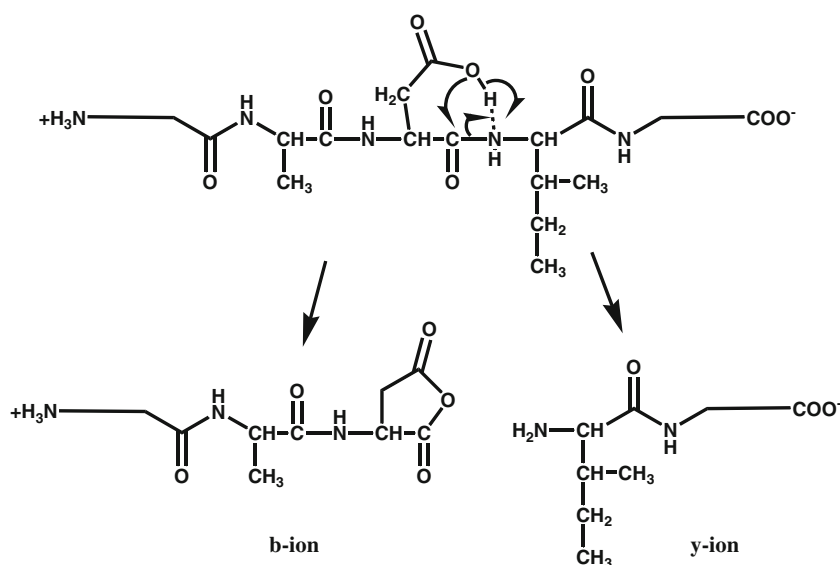
Scheme 4. Acid-initiated selective cleavage at peptide bond of Asp/Glu/Cys-Xxx residues

It is of importance to discuss the distinctions between selective/nonselective cleavage and the site of pos/neg charge. The nonselective cleavages that generate many b-ions reflect sequences observed in the positive ion CID spectra of the z′14 ion generated from cytochrome c and the z′15 ion from myoglobin. Both the z′14 and z′15 ions contain an Arg residue at the N-terminal side, indicative of the presence of positive charge attributable to protonated Arg at the N-terminal side. Although the mobile proton mechanism may be useful for interpreting the formation of a lot of b-ions, a series of y-ions (y_n, n = 5–12) observed in Figure 4a imply that Lys8 or Lys9 is also important for the site of positive charge on the product y-ions. The result described above suggests that the site of protonated residues is an important factor for observable product ions. In order to examine the relationships between the N-terminal side Arg residue and observable product ions, a model peptide ACTH18-39 was used for pos/neg ion CID experiments, which looked at analyte ions $[M + H]^+$ and $[M - H]^-$ (Supplemental Figure S3). The resulting major product ions are summarized in Table 3. The positive ion CID spectrum shows intense product b12, y20, and b12/y20 ions originating from preferential peptide bond cleavage at Asp-Glu, Pro-Val, and (Asp-Glu)/(Pro-Val) residues, respectively, and further, lower-abundance product b5, b6, b7, b8, b9, b10, b11, b13, b15, b16, b18, b21, y19, and y21 ions were also observed. The other product ions b14, b17, b19, b20, and y-ions (y_n, n < 18) were
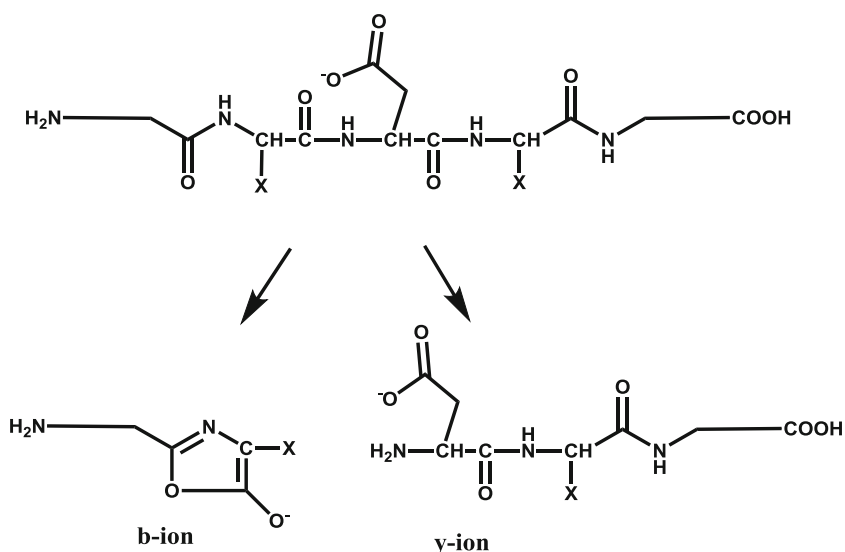
Scheme 5. Negative charge-initiated selective cleavage at peptide bond of Xxx-Asp/Glu/Cys residues

Table 3. Product Ions, Cleavage Sites, and Relative Intensity (%) Observed in Positive and Negative Ion CID Spectra of Analyte Ions $[M + H]^+$ and $[M - H]^-$ of ACTH18-39

Precursor	Major product ions (cleavage residues, relative intensity %)
$[M + H]^+$	b12 (D-E, 100)*, y20 (P-V, 46), b12/y20 (D-E/P-V, 36)
$[M - H]^-$	y11 (E-D, 100)* y10 (D-E, 97)*, y7 (A-E, 32)*

* Accompanied with the loss of neutrals such as NH_3 and/or H_2O

barely observed in the CID spectrum. Taking into account the two-factors influencing observable product ions [i.e., (1) the sites of charge and (2) the susceptibility of amino acid residues to CID] it can be assumed that Ser-Ala, Ala-Phe, Pro-Leu, and Leu-Glu residues for the product b14, b17, b19, and b20 ions are less susceptible to the low-energy CID, and that y-ions (y_n, n < 18) are hardly observed because of the absence of positive charge at the C-terminal side. The major product ions in the negative ion CID spectrum of ACTH18-39 summarized in Table 3 originate from cleavage at Xxx-Asp/Glu residues, accompanied by the loss of neutrals. Formation of these product ions might be rationalized by a negative charge-mediated cleavage mechanism (Scheme 5).

Influence of Secondary Structures on Product Ion Formation in CID Experiments

Although it is of particular interest to consider the influence of secondary structures of peptides on the CID experiments, it is difficult to obtain definite evidence for the presence of intramolecular hydrogen bonded secondary structures such as α-helix and β-sheet in a given analyte peptide under mass spectrometric gas-phase conditions. Here we describe pos/neg ion CID spectra of the c- and z′-ions generated from MALDI-ISD of intact proteins with definite secondary structures based on the X-ray and/or NMR data. The resulting CID product ions can be explained by selective cleavages adjacent to acidic Asp, Glu, and Cys residues, which are independent of the helix domains. However, the observation of extremely intense product ions y23 and y15 in the positive ion CID spectra of the c43 and c35 ions, respectively, generated from the MALDI-ISD of myoglobin (Figure 5) suggests that acidic residues lying in helix-free regions between two long helical domains tend to degrade more than those in helical regions. The absence of any readable product ions in the negative ion CID of the c43 and c35 ions may be due to the presence of α-helix in the c43 and c35 ions (Figure S2). The pos/neg ion CID spectra of a model peptide ACTH18-39, which produced a lot of product ions, were useful for estimating the influence of secondary structures on CID product ion formation because ACTH18-39 has no helical structures. Thus, the major product ions originating from selective cleavages adja-

cent to acidic residues and a lot of minor product ions originating from nonselective cleavages by the mobile proton mechanism may be a result of the helix free structure of ACTH18-39.

Conclusion

Ion trap low-energy CID experiments were performed for peptide fragment ions c- and z′-ions generated from MALDI-ISD of the intact proteins, equine holo-cytochrome *c* and equine apo-myoglobin. The MALDI-ISD spectra of the proteins gave discontinuous abundant fragment ions originating from N–Cα bond cleavages at Xxx-Asp, Xxx-Asn, and Gly-Xxx residues, independent of pos/neg ion experiments. The positive ion CID spectra of the c- and z′-ions characteristically showed that the product ions originated from selective cleavages at Asp-Xxx, Glu-Xxx, and Cys-Xxx residues independent of the sequences of the c- and z′-ions. The nonselective cleavage product ions which can be explained by the mechanism of "mobile proton" were also observed when a positively charged Arg residue was located on the N-terminal side, as well as the product ions produced by selective cleavages at the acidic residues Asp, Glu, and Cys. These selective and nonselective product ions were informative for the sequence analysis of the c- and z′-ions generated from MALDI-ISD experiments of proteins. In contrast, negative ion CID spectra of the ISD fragments resulted in product ions too complex to allow assignments. The observed negative product ions were almost always accompanied by the loss of neutrals from b-, c-, and y-ions. A characteristic feature of the negative ion CID was selective cleavages at the N-terminal side of the peptide bond of the acidic residues Asp, Glu, and Cys, Xxx-Asp/Glu/Cys (Scheme 5), whereas positive ion CID resulted in cleavages at Asp/Glu/Cys-Xxx residues (Scheme 4).

Although definite evidence for the influence of α-helix on the CID product ions of peptides was not obtained, the pos/neg ion CID of the c43 and c35 ions generated from the MALDI-ISD of intact myoglobin suggests that acidic residues lying in helix-free regions between two long α-helical domains tend to degrade more than those in helical regions. In contrast, pos/neg ion CID spectra of a model peptide ACTH18-39, which has a helix free structure showed the presence of a lot of product ions suggesting that selective and nonselective cleavage may be due to helix free structures.

References

1. Karas, M., Bachmann, D., Bahr, U., Hillenkamp, F.: Matrix-assisted ultraviolet laser desorption of non-volatile compounds. Int. J. Mass Spectrom Ion Process **78**, 53–68 (1987)
2. Tanaka, K., Waki, H., Ido, Y., Akita, S., Yoshida, Y., Yoshida, T.: Protein and polymer analyses up to *m/z* 100,000 by laser ionization time-of-flight mass spectrometry. Rapid Commun. Mass Spectrom. **2**, 151–153 (1988)
3. Whitehouse, C.M., Dreyer, R.N., Yamashita, M., Fenn, J.B.: Electrospray interface for liquid chromatographs and mass spectrometers. Anal. Chem. **57**, 675–679 (1985)
4. Fenn, J.B., Mann, M., Meng, C.K., Wong, S.F., Whitehouse, C.M.: Electrospray ionization for mass spectrometry of large biomolecules. Science **246**, 64–71 (1989)
5. Resemann, A., Wunderlich, D., Rothbauer, U., Warscheid, B., Leonhardt, H., Fuchser, J., Kuhlmann, K., Suckau, D.: Top-down de novo protein sequencing of a 13.6 kDa camelid single heavy chain antibody by matrix-assisted laser desorption/ionization-time-of-flight/time-of-flight mass spectrometry. Anal. Chem. **82**, 3283–3292 (2010)
6. Sellami, L., Belgacem, O., Villard, C., Openshaw, M.E., Barbier, P., Lafitte, D.: In-source decay and pseudo tandem mass spectrometry fragmentation processes of entire high proteins on a hybrid vacuum matrix-assisted laser desorption/ionization-quadrupole ion-trap time-of-flight mass spectrometer. Anal. Chem. **84**, 5180–5185 (2012)
7. Ait-Belkacem, R., Calligaris, D., Sellami, L., Villard, C., Granjeaud, S., Schembri, T., Berenguer, C., Ouafik, L., Figarella-Branger, D., Chinot, O., Lafitte, D.: Tubulin isoforms identified in the brain by MALDI in-source decay. J. Proteome **79**, 172–179 (2013)
8. Brown, R.S., Lennon, J.J.: Sequence-specific fragmentation of matrix-assisted laser-desorbed protein/peptide ions. Anal. Chem. **67**, 3990–3999 (1995)
9. Hardouin, J.: Protein sequence information by matrix-assisted laser desorption/ionization in-source decay mass spectrometry. Mass Spectrom. Rev. **26**, 672–682 (2007)
10. Calligaris, D., Villard, C., Terras, L., Braguer, D., Verdier-Pinard, P., Lafitte, D.: MALDI in-source decay of high mass protein isomers: application to α- and β-tubulin variants. Anal. Chem. **82**, 6176–6184 (2010)
11. Calligaris, D., Villard, C., Lafitte, D.: Advances in top-down proteomics for disease biomarker discovery. J. Proteom. **10**, 920–934 (2011)
12. Debois, D., Bertrand, V., Quinton, L., De Pauw-Gillet, M.-C., De Pauw, E.: MALDI-in source decay applied to mass spectrometry imaging: a new tool for protein identification. Anal. Chem. **82**, 4036–4045 (2010)
13. Rand, K.D., Bache, N., Nedertoft, M.M., Jorgensen, J.D.: Spatially resolved protein hydrogen exchange measured by matrix-assisted laser desorption ionization in-source decay. Anal. Chem. **83**, 8859–8862 (2011)
14. Takayama, M.: Flexible Xxx-Asp/Asn and Gly-Xxx Residues of equine cytochrome *c* in matrix-assisted laser desorption/ionization in-source decay mass spectrometry. Mass Spectrom. **1**(2), A0007 (2012)
15. Takayama, M.: Susceptible region of myoglobins to in-source decay using matrix-assisted laser desorption/ionization coupled with delayed extraction reflectron time-of-flight mass spectrometer. J. Mass Spectrom. Soc. Jpn. **50**, 304–310 (2002)
16. Takayama, M., Osaka, I., Sakakura, M.: Influence of secondary structure on in-source decay of protein inn matrix-assisted laser desorption/ionization mass spectrometry. Mass Spectrom. **1**(1), A0001 (2012)
17. Paizs, B., Suhai, S.: Fragmentation pathways of protonated peptides. Mass Spectrom. Rev. **24**, 508–548 (2005)
18. Barton, S.J., Whittaker, J.C.: Review of factors that influence the abundance of ions produced in a tandem mass spectrometer and statistical methods for discovering these factors. Mass Spectrom. Rev. **28**, 177–187 (2009)
19. Dongre, A.R., Jones, J.L., Somogyi, A., Wysocki, V.H.: Influence of peptide composition, gas-phase basicity, and chemical modification on fragmentation efficiency: evidence for the mobile proton model. J. Am. Chem. Soc. **118**, 8365–8374 (1996)
20. Gu, C., Tsaprailis, G., Breci, L., Wysocki, V.H.: Selective gas-phase cleavage at the peptide bond c-terminal to aspartic acid in fixed-charge derivatives of Asp-containing peptides. Anal. Chem. **72**, 5804–5813 (2000)
21. Huang, Y., Wysocki, V.H., Tabb, D.L., Yates III, J.R.: The influence of histidine on cleavage C-terminal to acidic residues in doubly protonated tryptic peptides. Int. J. Mass Spectrom. **219**, 233–244 (2002)
22. Tsaprailis, G., Nair, H., Somogyi, A., Wysocki, V.H., Zhong, W., Futrell, J.H., Summerfield, S.G., Gaskell, S.J.: Influence of secondary structure on the fragmentation of protonated peptides. J. Am. Chem. Soc. **121**, 5142–5154 (1999)
23. Bowie, J.H., Brinkworth, C.S., Dua, S.: Collision-induced fragmentations of the [M − H]⁻ parent anions of underivatized peptides: an aid to structure determination and some unusual negative ion cleavages. Mass Spectrom. Rev. **21**, 87–107 (2002)
24. Harrison, A.G.: Sequence-specific fragmentation of deprotonated peptides containing H or alkyl side chains. J. Am. Soc. Mass Spectrom. **12**, 1–13 (2001)
25. Pu, D., Cassady, C.J.: Negative ion dissociation of peptides containing hydroxyl side chains. Rapid Commun. Mass Spectrom. **22**, 91–100 (2008)
26. Pu, D., Clipston, N.L., Cassady, C.J.: A comparison of positive and negative ion collision-induced dissociation for model heptapeptides with one basic residue. J. Mass Spectrom. **45**, 297–305 (2010)
27. Demeure, K., Gabelica, V., De Pauw, E.A.: New advances in the understanding of the in-source decay in MALDI-TOF-MS. J. Am. Soc. Mass Spectrom. **21**, 1906–1917 (2010)
28. Asakawa, D., Sakakura, M., Takayama, M.: Influence of initial velocity of analytes on in-source decay products in MALDI mass spectrometry using salicylic acid derivative matrices. Int. J. Mass Spectrom. **337**, 29–33 (2013)
29. Osaka, I., Sakai, M., Takayama, M.: 5-Amino-1-naphthol, a novel 1,5-naphthalene derivative matrix suitable for matrix-assisted laser desorption/ionization in-source decay of phosphorylated peptides. Rapid Commun. Mass Spectrom. **27**, 103–108 (2013)
30. Takayama, M., Tsugita, A.: Does in-source decay occur independent of the ionization process in matrix-assisted laser desorption? Int. J. Mass Spectrom. **181**, L1–L6 (1998)
31. Williams, R.W., Chang, A., Juretic, D., Loughran, S.: Secondary structure predictions and medium range interactions. Biochim. Biophys. Acta **916**, 200–204 (1987)
32. Branden, C., Tooze, J.: Introduction to Protein Structure, pp. 11–29. Garland Publishing Inc, New York (1991)
33. Harrison, A.G., Young, A.B.: Fragmentation reactions of deprotonated peptides containing aspartic acid. Int. J. Mass Spectrom. **255**, 111–122 (2006)
34. Harrison, A.G., Young, A.B.: Fragmentation reactions of deprotonated peptides containing proline. The proline effect. J. Mass Spectrom. **40**, 1173–1186 (2005)
35. O'Connor, P.B., Lin, C., Cournoyer, J.J., Pittman, J.L., Belyayev, M., Budnik, B.A.: Long-lived electron capture dissociation product ions experience radical migration via hydrogen abstraction. J. Am. Soc. Mass Spectrom. **17**, 576–585 (2006)